

Direct Electrochemistry of Hemin on Graphdiyne Modified Carbon Ionic Liquid Electrode and Electrocatalysis to Bromate

Shiguan Xu¹, Lijun Yan¹, Hui Cheng¹, Hui Xie¹, Lina Zeng^{2,*}, Lin Li², Shuhai He³, Wei Sun^{1,*}

¹ Key Laboratory of Water Pollution Treatment and Resource Reuse of Hainan Province, Key Laboratory of Functional Materials and Photoelectrochemistry of Haikou, College of Chemistry and Chemical Engineering, Hainan Normal University, Haikou, 571158, P. R. China.

² Key Laboratory of Laser Technology and Optoelectronic Functional Materials of Hainan Province, College of Physics and Electronic Engineering, Hainan Normal University, Haikou 571158, P. R. China

³ Hainan Ecological Environmental Monitoring Center, 98 Baiju Avenue, Haikou 571126, China

*E-mail: sunwei@hainnu.edu.cn and zenglinahainan@126.com

Received: 28 July 2022 / Accepted: 19 September 2022 / Published: 10 October 2022

In this paper an electrochemical sensor was fabricated by dropping a graphdiyne (GDY) and hemin suspension solution on the surface of carbon ionic liquid electrode (CILE) followed by casting the Nafion film (Nafion/hemin-GDY/CILE). The morphology of GDY was observed by scanning electron microscopy with the biomolecular structure of hemin-GDY and hemin characterized by UV-Vis absorption spectrophotometry, which proved that hemin maintained the original structure after mixing with GDY. Direct electrochemistry of hemin on the GDY modified electrode was realized with a pair of well-defined redox peaks and electrochemical performances were checked in detail with the electrochemical parameters calculated. Nafion/hemin-GDY/CILE showed excellent electrocatalytic ability towards the reduction of bromate with the detection range from 5.00 to 50.0 mmol L⁻¹ and the detection limit of 3.3 mmol L⁻¹ (3 σ). In addition, the modified electrode possessed good reproducibility and stability, which was applied to the analysis of seawater samples.

Keyword: Hemin, Graphdiyne, Carbon ionic liquid electrode, Electrochemistry, Bromate.

1. INTRODUCTION

Electrochemical biosensors have been the research hotspot due to the high sensitivity and selectivity, small sample consumption, low cost, portability, ease of fabrication, and the capacity for high-throughput analysis [1]. In general, electrochemical biosensors are consisted of biomolecular recognition layer and electric signal conversion elements. The biomolecular recognition layer can be obtained by using a bio-sensitive substrate functionalized with molecular recognition entities such as

enzymes, cells, antibodies, nucleic acids, protein, etc [2-4]. Due to the excellent physicochemical properties of carbon nanomaterials such as large surface area, high conductivity and good biocompatibility, a variety of carbon based composites have been used to achieve protein electrochemistry with enhanced electrochemical response [5-8]. The presence of nanostructured carbon materials can overcome the electron transfer barriers between the active center of the protein and the electrode, and the fabricated electrochemical sensors show excellent electrocatalytic activity and sensing ability [9-11].

As new type of carbon nanomaterial with sp and sp^2 hybridized carbon atoms and a unique butadiyne bond ($-C\equiv C-C\equiv C-$) in the π conjugate structure, graphdiyne (GDY) exhibits specific properties including excellent electrical conductivity, efficient catalytic performance and good chemical stability [12-15]. Yan et al. applied GDY based nanocomposites for the electrochemical sensing of drugs with satisfactory results [16,17]. Inspired by the charming applications of GDY, herein a commonly used N-hexylpyridinium hexafluorophosphate (HPPF₆) based carbon ionic liquid electrode (CILE) was fabricated and modified by hemin and GDY composite to obtain a new modified electrode (Nafion/hemin-GDY/CILE). The electrochemical behavior of the modified electrode was investigated with a pair of redox peaks appeared, which was resulted from the direct electron transfer of hemin that had the same active center as peroxidase. The modified electrode was further investigated to sensitively detect bromate solution and seawater samples with satisfactory results.

2. EXPERIMENTAL

2.1 Chemicals and apparatus

CHI 660D electrochemical workstation (Shanghai CH instrument, China) was connected with a three-electrode model, which was made up of Nafion/hemin-GDY/CILE (the working electrode), saturated calomel electrode (SCE, the reference electrode) and platinum wire electrode (the counter electrode). UV-5 ultraviolet-visible spectrophotometer (Mettler Toledo, USA) and JSM-7100F scanning electron microscopy (SEM, JEOL, Japan) were used for characterization.

Graphdiyne (GDY, Nanjing XFNANO Materials Tech. Ltd. Co., China), Nafion (5.0-5.4 wt%, Dupont, USA), hemin (Sigma-Aldrich Co., USA), N-hexylpyridinium hexafluorophosphate (HPPF₆, Lanzhou Yulu Fine Chem. Ltd. Co., China) and bromate (Shanghai Aladdin Reagent Ltd. Co., China) were used as received. The supporting electrolyte was 0.1 mol L⁻¹ phosphate buffer solution (PBS), which was deoxygenized by purging with nitrogen for 10 min before the experiment and all measurements were carried out at room temperature.

2.2 Fabrication of modified electrode

CILE was prepared with graphite powder and HPPF₆, which was used as the basic electrode [18]. Then, 4.0 μ L of a mixed solution containing 0.5 mg mL⁻¹ GDY and 15.0 mg mL⁻¹ hemin was applied on the surface of CILE. After drying at room temperature, 6.0 μ L of 0.5% Nafion solution was further

spread on the electrode surface to fabricate the working electrode (Nafion/hemin-GDY/CILE), which was stored at 4°C before used. Other electrodes were fabricated by the similar procedure for comparison.

2.3 Electrochemical procedure

Electrochemical behaviors of different modified electrodes were investigated by cyclic voltammetry (CV), which was performed in the potential range between -0.2 and 0.8 V at the scan rate of 100 mV s⁻¹.

3. RESULTS AND DISCUSSIONS

3.1. Characterizations

SEM images of GDY at different magnifications were displayed in Fig. 1. It can be seen that GDY shows rough surface and thin layered fold structure (Fig. 1A), which is typical two-dimensional structure of GDY [19]. As shown in Fig. 1B, GDY at high resolution exhibits wrapped and agglomerated microstructure, which is ascribed to the π - π stacking affinity.

UV-Vis absorption spectroscopy is a common method to investigate the secondary structure of the proteins. According to the position of the protein absorption band, it could be judged whether the structure of hemin had changed [20]. Fig. 1C showed the UV-Vis spectra of hemin in water (curve a) and hemin-GDY mixture solution (curve b), which gave the same typical Soret band of hemin at 375 nm. The result indicated that hemin had not been denatured after mixing with GDY and maintained the original biological structure.

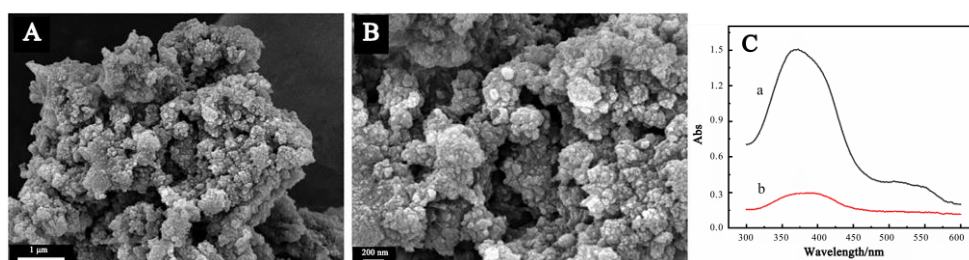


Figure 1. (A, B) SEM images of GDY at different magnifications; (C) UV-Vis absorption spectra of hemin (a) and the mixture of hemin-GDY solution (b).

3.2 Direct electrochemistry of Hb

Fig.2 showed the CV curves of different modified electrodes in pH 6.5 PBS. On Nafion/CILE (curve a) and Nafion/GDY/CILE (curve b), no redox peaks were observed within the potential window, indicating no electrochemical reaction occurred on the electrode surface. However, the presence of GDY on CILE surface resulted in the increase of background currents due to its large surface area. As for Nafion/hemin/CILE (curve c), a pair of small redox peaks appeared, proving the electron transfer

between redox active center of hemin and CILE could be realized with slow rate. After the electrode surface was modified with GDY, the redox peak currents increased on Nafion/hemin/GDY/CILE (curve d), indicating that the presence of GDY was benefit for the direct electron transfer between hemin and the electrode. However, on Nafion/hemin-GDY/CILE (curve e), the redox peak currents were bigger than that of Nafion/hemin/GDY/CILE, indicating that mixing of GDY with hemin led to a higher electron transfer rate. The reason may be due to close interact of GDY nanosheet with hemin molecule after mixture that can decrease the electron transfer path. The values of E_{pc} and E_{pa} were got as -0.429 V and -0.264 V with the peak-to-peak separation (ΔE_p) as 165 mV, and the formal peak potential (E^0) was -0.347 V (vs. SCE). Also, the redox peak currents were recorded as I_{pc} ($182 \mu\text{A}$) and I_{pa} ($217 \mu\text{A}$) with the value of I_{pc}/I_{pa} as 0.94 . All the results indicated that the characteristic electrochemical behavior of hemin Fe (III)/Fe (II) was realized with an approximately reversible process Hemin has the same active center as peroxidase with Fe (III)/Fe (II) redox couples, which can take place the direct electrochemistry reaction at optimal experimental conditions [21].

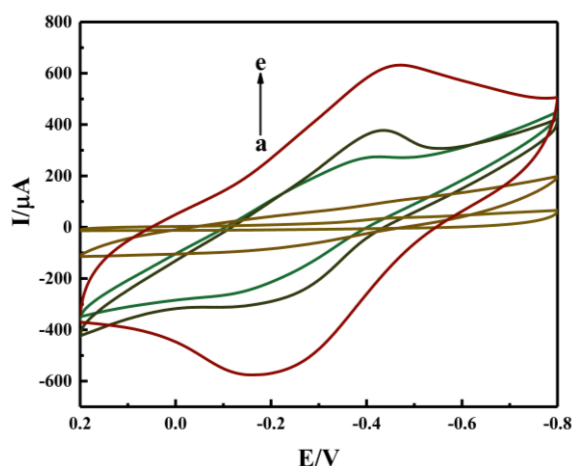


Figure 2. Cyclic voltammograms of (a) Nafion/CILE, (b) Nafion/GDY/CILE, (c) Nafion/hemin/CILE, (d) Nafion/hemin/GDY/CILE, (e) Nafion/hemin-GDY/CILE in pH 6.5 PBS with scan rate as 100 mV s^{-1} .

3.3 Effect of scan rate

Electrochemical responses of Nafion/hemin-GDY/CILE were investigated at different scan rate with curves shown in Fig. 3A. The cathodic and anodic peak currents of hemin increased gradually with the increase of scan rate (Fig. 3B). Two linear regression equations were obtained as $I_{pa} (\mu\text{A}) = -1567 v (\text{V s}^{-1}) - 50.7$ ($n=10, \gamma=0.994$) and $I_{pc} (\mu\text{A}) = 776 v (\text{V s}^{-1}) + 48.5$ ($n=10, \gamma=0.993$), respectively, indicating a typical interface-dominated process due to the immobilization of hemin on the electrode surface. With the increase of scan rate, ΔE_p also increased (Fig. 3C) and two linear relationships were got with the regression equations as $E_{pc} (\text{V}) = -0.0620 \ln v (\text{V s}^{-1}) - 0.523$ ($n=10, \gamma=0.999$) and $E_{pa} (\text{V}) = 0.0873 \ln v (\text{V s}^{-1}) - 0.00668$ ($n=10, \gamma=0.999$), respectively. According to Laviron's equation [22], the electron transfer coefficients (α) and the reaction rate constant (k_s) were calculated as 0.698 and 0.248 .

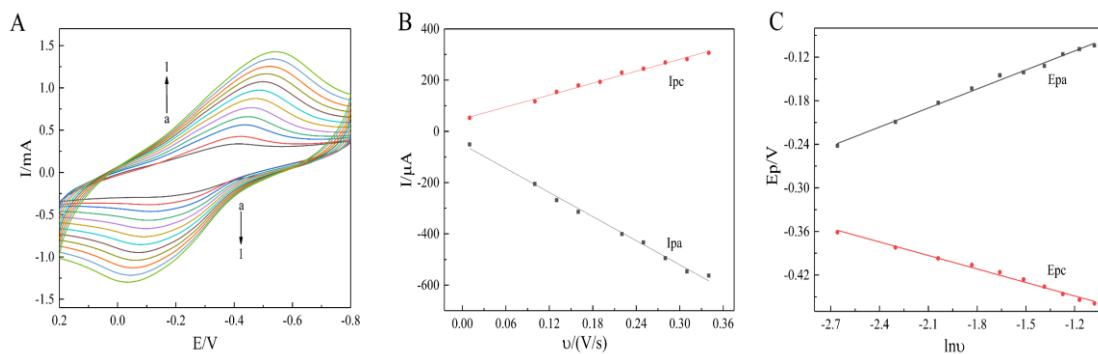


Figure 3. (A) Cyclic voltammograms of Nafion/hemin-GDY/CILE in pH 6.5 PBS with different scan rates (from a to l as 0.04, 0.07, 0.10, 0.13, 0.16, 0.19, 0.22, 0.25, 0.28, 0.31, 0.34, 0.37 $V s^{-1}$); (B) Linear relationship of redox peak currents versus scan rate (v); (C) Linear relationship of redox peak potentials versus $\ln v$.

3.4 Effect of pH

Fig. 4A displayed the cyclic voltammograms of Nafion/hemin-GDY/CILE in 0.1 mol L^{-1} PBS at different pH values from 5.0 to 7.5. The negative shift of redox peak potentials was observed with the increase of pH, indicating that the proton participated in electrochemical process of Fe (III)/Fe (II). As shown in Fig. 4B, the linear regression equation of the formal peak potential ($E^{0'}$) and pH was calculated as $E^{0'} (V) = -0.0543 \text{ pH} + 0.0329$ ($n=6$, $\gamma=0.997$). The slope of -54.3 mV pH^{-1} was close to the theoretical value of -59 mV pH^{-1} for proton-coupled electron transfer process. Therefore, the electrochemical reaction could be expressed with the equation as $\text{hemin Fe (III)} + \text{H}^+ + e \rightarrow \text{hemin Fe (II)}$. In addition, the biggest redox peaks appeared at pH 6.5 buffer solution, which was used for all the electrochemical investigations.

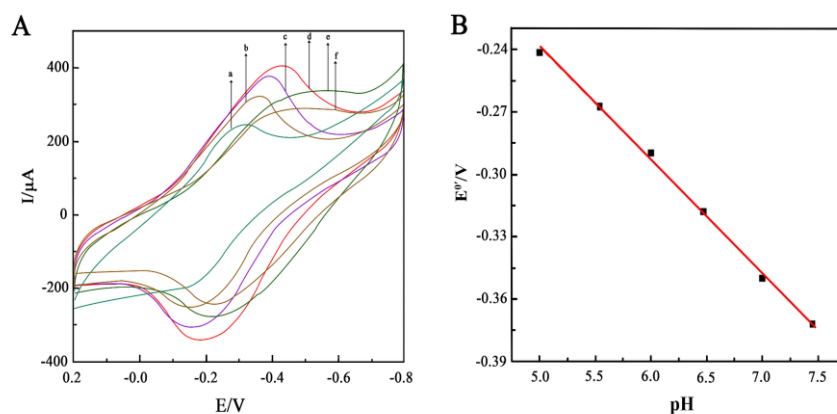


Figure 4. (A) Cyclic voltammograms of Nafion/hemin-GDY/CILE in different pH values (from a to f as 5.0, 5.5, 6.0, 6.5, 7.0, 7.5) with the scan rate of 100 $mV s^{-1}$; (B) Linear relationship of $E^{0'}$ with buffer pH.

3.5 Electrocatalytic behaviors

Hemin has the same redox center as peroxidase and can catalyze the reduction of bromate, which is used to estimate the performance of this hemin modified electrode [23]. CV curves of Nafion/hemin-

GDY/CILE after the gradually additions of bromate standard solution were recorded (as shown in Fig. 5). As the concentration increased, the corresponding reduction current (I_{pc}) also increased. The linear relationship between the reduction peak current and bromate concentration was got in the range of 5.00 to 50.0 $\text{mmol}\cdot\text{L}^{-1}$ (Inset of Fig. 5) with the regression equation as $I_{pc} (\mu\text{A}) = 25.3 C (\text{mmol L}^{-1}) + 232$ ($n=17, \gamma=0.995$) and the detection limit as $3.3 \text{ mmol L}^{-1} (3\sigma)$. The comparison of the analytical results with other modified electrodes is listed in table 1, which demonstrated that this modified electrode has comparable performances for bromate analysis.

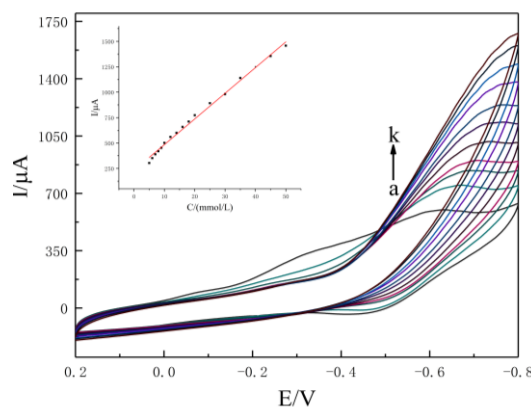


Figure 5. Cyclic voltammograms of Nafion/hemin-GDY/CILE with different concentrations of bromate (from a to k as: 5.0, 8.0, 12.0, 16.0, 20.0, 25.0, 30.0, 35.0, 40.0, 45.0, 50.0 mmol L^{-1}), inset is the linear relationship of reduction peak current versus bromate concentration.

Table 1. Comparison of various modified electrodes for bromate detection.

| Electrodes | Detection limit (mmol L^{-1}) | Linear range (mmol L^{-1}) | Ref. |
|--|--|---------------------------------------|-----------|
| Nafion/HRP/AuNPs-CCNTs/CILE | 0.16 | 0.5-10.0 | 21 |
| Nafion/Hb/HGNs/ CILE | 0.04 | 0.1-9.5 | 24 |
| Nafion/Hb/AuNPs/ND/CILE | 0.0033 | 0.01-12.0 | 25 |
| Nafion/Hb/Au/ZIF-8/CILE | 0.16 | 0.5-10.0 | 26 |
| Nafion/Hb/Pt-FeP-C/CILE | 0.25 | 0.76-7.00 | 27 |
| Nafion/Hb/ Co_3O_4 -CNF/CILE | 0.033 | 0.1-48 | 28 |
| Nafion/hemin-GDY/CILE | 3.30 | 5.0-50.0 | This work |

3.6 Sample detection

The determination of bromate content in the filtered seawater collected from Guilinyang Beach of Haikou city was investigated. Also, different standard bromate solutions were added to the sample solutions for the recovery test, and the results were calculated by the calibration curve with the recovery by the standard addition method. As shown in Table 2, the detection results were satisfactory with the recovery in the range of 92.48% to 109.69%, indicating the practical application of this method.

Table 2. Analytical data of bromate concentrations in seawater samples (n=3).

| Sample | Detected (mmol L ⁻¹) | Added (mmol L ⁻¹) | Total (mmol L ⁻¹) | Recovery (%) | RSD (%) |
|----------|-------------------------------------|----------------------------------|----------------------------------|-----------------|------------|
| Seawater | 0 | 20.00 | 18.49 | 92.48 | 6.06 |
| | | 30.00 | 30.39 | 101.30 | 4.40 |
| | | 40.00 | 43.88 | 109.69 | 2.52 |

3.7 Stability

The storing stability of the modified electrode was investigated by cyclic voltammetry in the pH 6.5 PBS, which was kept at 4°C refrigerator and measured over two weeks period. It was found that the current responses remained 95.62% of the original value. The good long-term stability might be ascribed to the stability of GDY that providing an excellent microenvironment for hemin to keep its bioactivity. After 40 circles cyclic voltammetric scan at scan rate of 100 mV s⁻¹, the redox peak currents remained 93.21% of the original current, also indicating the modified electrode had good using stability.

4. CONCLUSION

In this study, GDY was used as a new modifier on electrode to construct a simple hemin-based electrochemical sensor. Due to the good electrical conductivity and chemical stability of GDY, the electron transfer rate of hemin on the electrode surface was significantly increased with the bigger redox peak currents. The modified electrode was used to detect bromate with good electrocatalytic performance, including excellent stability, wider linear range, and lower detection limit. All results showed that GDY could be used for electrode modification and signal amplification, which had potential application prospects in the field of electrochemical sensing.

ACKNOWLEDGEMENTS

This project was supported by the This work is supported by Hainan Provincial Natural Science Foundation (2019RC192), Science and Technology project of Hainan Province (ZDYF2020217), the Open Foundation of Key Laboratory of Laser Technology and Optoelectronic Functional Materials of Hainan Province (2022LTOM01).

References

1. F.A. Armstrong, G.S, *Electrochim. Acta*, 45 (2000) 2623.
2. X.L. Niu, W. Chen, X.L. Wang, Y.L. Men, Q. Wang, W. Sun, G.J. Li, *Microchim. Acta*, 185 (2018) 167.
3. S.Y. Dong, Q.X. Yang, Y.L. Fu, D.D. Zhang, T.L. Huang, *J. Solid State Electrochem.*, 22 (2018) 1689.
4. X.L. Niu, H. Xie, G.L. Luo, Y.L. Men, W.L. Zhang, W. Sun, *J. Electrochem. Soc.*, 165 (2018) B713.
5. W. Chen, X.L. Niu, X.Y. Li, X.B. Li, G.J. Li, B.L. He, Q.T. Li, W. Sun, *Mater. Sci. Eng. C*, 80 (2017) 135.

6. S.W. Zhang, T.W. Ma, H. Zeng, F. Wang, *Polym. Mater.*, 31 (2021) 741.
7. L. Zhu, X.Y. Li, Y. Deng, R.Y. Zou, B. Shao, L.Y. Yan, C.X. Ruan, W. Sun, *J. Iran. Chem. Soc.*, 18 (2021) 1027.
8. H.A. Yones, L. Zhu, B. Shao, S.Y. Zhang, H. Xie, X.Q. Li, W. Sun, *Int. J. Electrochem. Sci.*, 16 (2021) 210225.
9. X.J. Liu, W.W. Chen, M.L. Lian, X. Chen, Y.L. Lu, W.S. Yang, *J. Electroanal. Chem.*, 833 (2019) 505.
10. J. Filip, A. Andicsová-Eckstein, A. Vikartovská, J. Tkac, *Biosens. Bioelectron.*, 89 (2017) 384.
11. Y.X. Sun, W. Chen, X.Q. Li, Q.Y. Yu, Y.X. Zhu, Y.T. Wang, L. Chen, W. Sun, G.J. Li, Y.Y. Niu, *Int. J. Electrochem. Sci.*, 16 (2021) 211050.
12. S. Pooja, M. Parteek, K. Vineet, S. Mika, *Sep. Purif. Technol.*, 281 (2022) 119825.
13. Y.S. Zhao, H.J. Tang, N.L. Yang, D. Wang, *Adv. Sci.*, 5 (2018) 1800959.
14. H.H. Wong, M.Z. Sun, B.L. Huang, *Chem. Res. Chin. Univ.*, 37 (2021) 1242.
15. H.Y. Yao, Y.S. Zhao, N.L. Yang, W. Hao, H. Zhao, S.Z. Li, J. Zhu, L. Shen, W. H. Fang, *J. Energy Chem.*, 65 (2022) 141.
16. L.J. Yan, T.X. Hu, X.Q. Li, F.Z. Ding, B. Wang, B.L. Wang, B.X. Zhang, F. Shi, W. Sun, *Electroanalysis*, 34 (2022) 286.
17. L.J. Yan, L.F. Huang, T.X. Hu, Y.J. Ai, B. Wang, W. Sun, *Talanta*, 242 (2022) 123295.
18. W. Chen, W. Weng, X. Niu, X. Li, Y. Men, W. Sun, G. Li, L. Dong, *J. Electroanal. Chem.*, 823 (2018) 137.
19. G.X. Li, Y.L. Li, H.B. Liu, Y.B. Guo, Y.J. Li, D.B. Zhu, *Chem. Commun.*, 46 (2010) 3256.
20. K. Rosenheck, P. Doty, *Proceedings of the National Academy of Sciences*, 47 (1961) 1775.
21. Y.C. Yao, C.X. Yin, S.G. Xu, M. Jiang, L. Zhu, R.Y. Zou, W. Sun, *Int. J. Electrochem. Sci.*, 17 (2022) 220546.
22. E. Laviron, *J. Electroanal. Chem.*, 101 (1979) 19.
23. X.Y. Li, G.L. Luo, H. Xie, Y.Y. Niu, X.B. Li, R.Y. Zou, Y.R. Xi, Y. Xiong, W. Sun, G.J. Li, *Microchim. Acta*, 186 (2019) 304.
24. X.Q. Li, B. Shao, Y.X. Sun, B.X. Zhang, X.H. Wang, W. Sun, *Int. J. Electrochem. Sci.*, 16 (2021) 210219.
25. H. Cheng, Y.X. Sun, B. Shao, Y. Deng, X.P. Zhang, G.J. Li, W. Sun, *Int. J. Electrochem. Sci.*, 15 (2020) 11416.
26. J. Liu, W.J. Weng, C.X. Yin, G.L. Luo, H. Xie, Y.Y. Niu, X.Y. Li, G.J. Li, Y.R. Xi, Y.T. Gong, S.Y. Zhang, W. Sun, *Int. J. Electrochem. Sci.*, 14 (2019) 1310.
27. F. Shi, H. Cheng, Y.C. Yao, Z.J. Zhang, L.N. Zeng, L. Li, W. Sun, *Int. J. Electrochem. Sci.*, 17 (2022) 220840.
28. H. Xie, G.L. Luo, Y.L. Niu, W.J. Weng, Y.X. Zhao, Z.Q. Ling, C.X. Ruan, G.J. Li, W. Sun, *Mater. Sci. Eng. C.*, 107 (2020) 110209.